

Database of superconductors with kagome lattice by high-throughput screening

Lihong Wang(王历宏), Qi Li(李琦), Ke Ma(马克), Yingpeng Yu(于英鹏), Shifeng Jin(金士锋), and Xiaolong Chen(陈小龙)

Citation: Chin. Phys. B, 2025, 34 (**10**): 106101. DOI: 10.1088/1674-1056/adf041
http://cpb.iphy.ac.cn; http://iopscience.iop.org/cpb

What follows is a list of articles you may be interested in

General-purpose moment tensor potential for Ga-In liquid alloys towards large-scale molecular dynamics with *ab initio* accuracy

Kai-Jie Zhao(赵凯杰) and Zhi-Gong Song(宋智功)
Chin. Phys. B, 2025, 34 (**6**): 066101. DOI: 10.1088/1674-1056/adc661

Exploring superconductivity in dynamically stable carbon-boron clathrates trapping molecular hydrogen

Akinwumi Akinpelu, Mangladeep Bhullar, Timothy A. Strobel, and Yansun Yao
Chin. Phys. B, 2025, 34 (**3**): 036103. DOI: 10.1088/1674-1056/ada757

Database of ternary amorphous alloys based on machine learning

Xuhe Gong(巩旭菏), Ran Li(李然), Ruijuan Xiao(肖睿娟), Tao Zhang(张涛), and Hong Li(李泓)
Chin. Phys. B, 2025, 34 (**1**): 016101. DOI: 10.1088/1674-1056/ad8ec8

Visualizing extended defects at the atomic level in a $Bi_2Sr_2CaCu_2O_{8+\delta}$ superconducting wire

Kejun Hu(胡柯钧), Shuai Wang(王帅), Boyu Li(李泊玉), Ying Liu(刘影), Binghui Ge(葛炳辉), and Dongsheng Song(宋东升)
Chin. Phys. B, 2024, 33 (**9**): 096101. DOI: 10.1088/1674-1056/ad6ccd

Databases of 2D material-substrate interfaces and 2D charged building blocks

Jun Deng(邓俊), Jinbo Pan(潘金波), and Shixuan Du(杜世萱)
Chin. Phys. B, 2024, 33 (**2**): 026101. DOI: 10.1088/1674-1056/ad0626

DATA PAPER

Database of superconductors with kagome lattice by high-throughput screening

Lihong Wang(王历宏)[1,2,†], Qi Li(李琦)[1,2,†], Ke Ma(马克)[1,2], Yingpeng Yu(于英鹏)[1,2], Shifeng Jin(金士锋)[1,3,‡], and Xiaolong Chen(陈小龙)[1,3,§]

[1] *Institute of Physics, Chinese Academy of Sciences, Beijing* 100190, *China*
[2] *College of Materials Science and Opto-Electronic Technology, University of Chinese Academy of Sciences, Beijing* 101408, *China*
[3] *School of Physical Sciences, University of Chinese Academy of Sciences, Beijing* 101408, *China*

(Received 15 May 2025; revised manuscript received 14 July 2025; accepted manuscript online 16 July 2025)

The kagome lattice, characterized by a hexagonal arrangement of corner-sharing equilateral triangles, has garnered significant attention as a fascinating quantum material system that hosts exotic magnetic and electronic properties. The identification and characterization of this class of materials are critical for advancing our understanding of their role in emergent phenomena such as superconductivity. In this study, we developed a high-throughput screening framework for the systematic identification and classification of superconducting materials with kagome lattices, integrating them into established materials databases. Leveraging the Materials Project (MP) database and the MDR SuperCon dataset, we analyzed over 150000 inorganic compounds and cross-referenced 26000 known superconductors. Using geometry-based structural modeling and experimental validation, we identified 129 kagome superconductors belonging to 17 distinct structural families, many of which had not previously been recognized as kagome systems. The materials are further classified into three categories in terms of topological flat bands, clean band structures, and coexisting magnetic or charge density wave (CDW) orderings. Based on these results, we established a database comprising 129 kagome superconductors, including the detailed crystallographic, electronic, and superconducting properties of these materials.

Keywords: superconductor, kagome lattice, database

PACS: 61.68.+n, 74.25.–q

DOI: 10.1088/1674-1056/adf041 **CSTR:** 32038.14.CPB.adf041

1. Introduction

The kagome lattice consists of two-dimensional (2D) corner-sharing equilateral triangles arranged in a hexagonal pattern. It is an attractive quantum system that hosts exotic magnetic and electronic properties. A simple tight-binding model applied to this hexagonal network reveals highly unusual electronic structures, such as the presence of Dirac points, van Hove singularities, and topological flat bands. To date, several materials have been discovered to possess the kagome lattice and to exhibit novel kagome physics. For instance, the Fe kagome lattice within Fe_3Sn_2 demonstrates remarkable spin-orbit tunability,[1,2] while kagome $Co_3Sn_2S_2$ has been identified as a host for long-sought magnetic Weyl semimetals.[3] Additionally, kagome materials such as FeGe, which exhibits intertwined antiferromagnetism and charge density waves (CDW),[4] display a plethora of intriguing phenomena arising from complex quantum interactions between different electronic orders.[5,6] These unique characteristics make the kagome lattice an ideal platform for exploring novel quantum phenomena, ranging from spin liquids and superconductivity to topological magnetism and unconventional CDW.

Recently, AV_3Sb_5 (A = K, Rb, Cs) has attracted intense interest as a family of kagome superconductors.[7–12] These materials exhibit 2D kagome planes of V atoms separated by Sb layers. Superconductivity emerges below 2–4 K, and a CDW transition occurs around 100 K, highlighting the interplay between electronic correlations and lattice geometry in these compounds. Aside from the AV_3Sb_5 family, however, experimentally realized kagome superconductors remain limited. Recent theoretical studies have explored extensive element substitution within the AV_3Sb_5 structural prototype, predicting 28 potential kagome materials with similar structures.[13] With the rapid development of high-quality experimental databases and advanced computational tools, high-throughput materials screening and calculations have gained prominence in the field of materials science.[14] Recent efforts utilizing high-throughput screening and database-driven calculations have led to the discovery of stable and synthesizable kagome materials that may exhibit properties such as topological flat bands[15] and quantum spin liquid (QSL) behavior.[16] Therefore, expanding the scope of synthesizable supercon-

[†]These authors contributed equally to this work.
[‡]Corresponding author. E-mail: shifengjin@iphy.ac.cn
[§]Corresponding author. E-mail: chenx29@iphy.ac.cn
© 2025 Chinese Physical Society and IOP Publishing Ltd. All rights, including for text and data mining, AI training, and similar technologies, are reserved.

ducting materials through high-throughput screening is crucial for advancing research in kagome superconductors.

The MDR SuperCon dataset[17] compiles data on over 26000 experimentally confirmed superconductors, encompassing their chemical formulas, superconducting transition temperatures, and original references. On the other hand, the Materials Project (MP)[18] is a high-quality computational database that includes most of the stoichiometric crystal structures from the inorganic crystal structure database (ICSD), while also incorporating calculated and theoretically stable structures. In this work, we first employed geometry-based models to screen about 3800 synthesizable kagome materials from a pool of over 150000 materials to systematically search for experimentally synthesizable kagome superconductors. The results aligned closely with the $\sim$ 3500 experimental kagome entries reported from the ICSD in prior work.[19] This consistency in scale, derived from two large but distinct databases, provides strong support for the effectiveness of our geometric search algorithm. The results were then cross-referenced with the MDR SuperCon database by combining structural and superconducting properties. As shown in Fig. 1, these candidates were further compared with experimentally observed superconductors (in the SuperCon database) to identify materials common to both datasets (Fig. 1). We successfully identified 129 kagome superconductors belonging to 17 distinct structural types, many of which had been overlooked as kagome materials. Among these superconductors, we further classified kagome materials exhibiting interesting band structures or with intertwined magnetic or CDW orders, which may become focal points of current research. These newly identified compounds pave the way for more rigorous synthetic efforts and provide parent compounds for further chemical modifications.

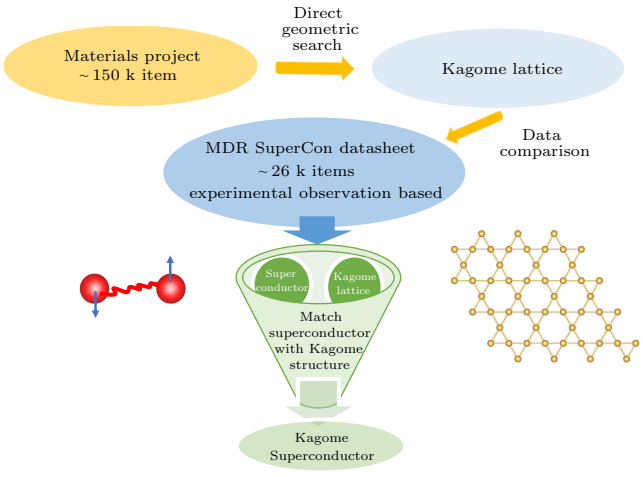


Fig. 1. Workflow for screening kagome superconductors using the Materials Project and MDR SuperCon databases.

2. Data acquisition

The search for kagome lattices in inorganic materials has been conducted through the use of unique Wyckoff positions with geometric constraints,[15,16] elemental substitution within specific chemical formulas,[13,20] or the implementation of direct geometric constraints on neighboring atoms.[19] In this work, we use a more comprehensive approach to constrain the kagome lattice through direct geometric measures, which also allows the identification of breathing kagome lattices. First, we target candidate atoms of a specific chemical element, identify their four nearest neighbors, and calculate the bond angles between them. The angles are constrained to $60^\circ \pm \delta$, $120^\circ \pm \delta$, and $180^\circ \pm \delta$ ($\delta = 0.1^\circ$). These atoms should form two corner-sharing triangles within a plane, allowing us to differentiate between normal kagome lattices, composed of congruent triangles, and breathing kagome lattices, where the triangles have unequal lengths. We then verify whether all atoms within this geometric plane satisfy the same criteria so that the structure can be recognized as a kagome layer. We also verify the corner-sharing triangles to distinguish normal kagome lattices, with congruent triangles (equal edge lengths), from breathing kagome lattices, with non-congruent triangles (distinct edge lengths). Subsequently, we confirm planarity (RMSD < 0.1 Å) and validate that all atoms in the layer satisfy the previous criteria. Finally, we check whether atoms within this plane are shared between multiple kagome layers — indicating that the layers intersect and the material is not two-dimensional. If this condition is met, the compound is classified as a 'crossed kagome' material with three-dimensional (3D) interpenetrating layers. Otherwise, it is designated as a 'separated kagome' material, which has no shared atoms, and we determine the number of distinct kagome layers within the unit cell along with their interlayer distances. The geometric search method is carried out mainly with the Pymatgen package.[21]

The initial structure search yielded over 10000 kagome lattices, including both experimentally observed and theoretical structures. By excluding the theoretical structures, the number of kagome lattices decreased to approximately 3800. Subsequently, we integrated the results with the MDR SuperCon dataset by matching chemical formulas and structure types, followed by manual correction. The dataset provides not only crystal structure information but also physical properties sourced mainly from the MP database, such as thermodynamic stability,[22–24] magnetic properties,[25] and electronic structure.[26] The screened materials are provided in the supporting information as a CSV file, and the corresponding band structures obtained from the MP database are also presented. Additionally, some newly identified kagome superconductors not previously recorded in the databases are included.

To demonstrate the presence of flat bands, we analyzed the electronic structures of two selected kagome superconductors, $BaNbS_3$ and La_3Al, using density functional theory (DFT) calculations implemented in the Vienna *ab initio* software package (VASP).[27] The projector augmented-wave (PAW) method and the Perdew–Burke–Ernzerhof (PBE) exchange–correlation functional were employed for these calculations. The plane-wave energy cutoff was set to 600 eV, and the energy convergence criterion was set to 1×10^{-6} eV. An $8 \times 8 \times 10$ k-mesh was used for Brillouin zone sampling.

3. Detail of database

3.1. Crystallographic classification of kagome superconductors

The database comprises a total of 129 synthesizable kagome superconductors with well-defined structures. Among these, 123 were identified by screening a combination of the kagome database and the superconductor databank, while the remaining 6 were added from recent literature. All entries have been systematically classified and categorized. As shown in Fig. 2, the screened kagome superconductors exhibit a diverse range of space groups and prototypes, which can be grouped into 17 structural prototypes. These prototypes are confined to the hexagonal, trigonal, and cubic crystal systems, with cubic kagome superconductors being the most prevalent. Specifically, 58 superconductors are found in the *R*-3*m*, *P*6/*mmm*, and *P*6$_3$/*mmc* space groups, which correspond to compounds with spatially separated kagome layers. In addition, 71 superconductors featuring a crossed kagome lattice fall into the cubic *P*-3*m*, *Pm*-3*m*, and *Fd*-3*m* space groups. In terms of chemical composition, the binary compounds AB_2 and AB_3 are the most common anonymized formulas, corresponding to laves-$MgZn_2$, laves-$MgCu_2$, and Cu_3Au prototypes, respectively. Notably, all screened kagome superconductors possess spatial inversion symmetry. In addition, no quaternary kagome superconductors were identified in our screening.

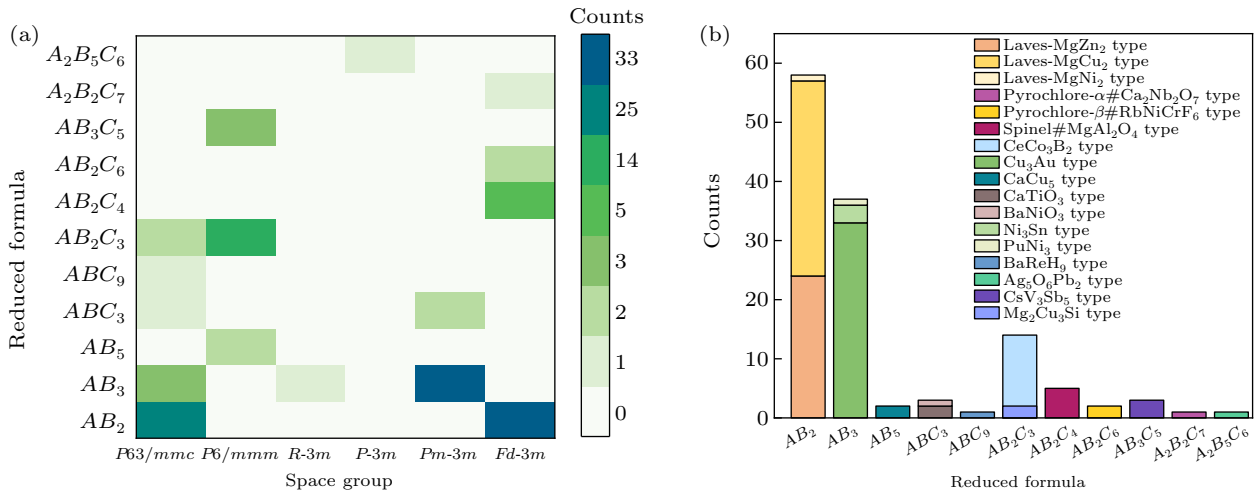


Fig. 2. Structural classification of kagome superconductors. (a) Heat map showing the distribution of materials by reduced chemical formula (rows) and space group (columns), where the color intensity of each box represents the number of compounds. (b) Histogram showing the frequency of materials categorized by reduced formula and structural type.

3.1.1. Superconductors with separate kagome layers

This category in the database includes superconductors that host separate kagome layers. The screened superconductors, in which the kagome net is separated by other atomic layers, are potential hosts of clean kagome bands. These superconductors crystallize exclusively in three hexagonal and trigonal space groups: *R*-3*m*, *P*6/*mmm*, and *P*6$_3$/*mmc*. Figure 3 illustrates representative kagome superconductors with only one kagome layer in each unit cell, which belong to the same category as some of the best-known kagome superconducting materials such as RV_3Sb_5 (R = K, Rb, Cs).

The kagome superconductors in the $CaCu_5$ prototypes (abbreviated as AB_5) consist of only two atomic layers within a unit cell, making them the smallest and simplest examples of kagome superconductors. In the AB_5 compounds $ThIr_5$ and $BaAu_5$, the three B atoms form a 2D kagome net sandwiched between the AB_2 block layers. By replacing the two B atoms in the AB_2 block layers with a third element, another kagome superconducting family in the $CeCo_3B_2$ prototype (abbreviated as AB_3C_2) is formed, hosting up to 14 different superconductors — the second largest in non-cubic systems (Fig. 2). Compared to AB_5, the elimination of common atoms in the block layer of AB_3C_5 helps reduce impurity bands.

Additionally, the RV_3Sb_5 (R = K, Rb, Cs) superconductors consist of V–Sb slabs intercalated by alkali-metal cations, with the vanadium sublattice forming a structurally perfect 2D kagome net. The introduction of alkali-metal layers ensures that the 2D V–Sb kagome nets are chemically isolated from one another, resulting in clean kagome energy bands. The last superconductor with a single 2D kagome layer in a unit cell in

Fig. 3 is $Ag_5O_6Pb_2$. The structure resembles the AB_5 structure type, where two Ag atoms in the block layers are adjacent to three Ag atoms forming the 2D kagome net.

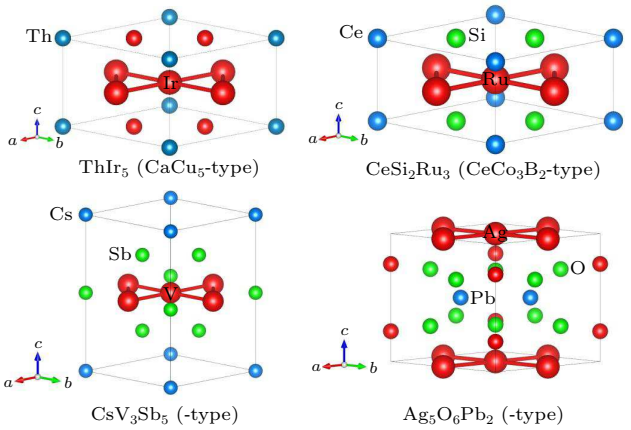


Fig. 3. Crystal structure of superconductors with a single kagome layer in a unit cell. Red atoms indicate intralayer bonds within the kagome plane.

In Fig. 4, we present more complex superconductors that host multiple kagome layers within a single unit cell. Notably, all these multilayer kagome superconductors belong to the breathing kagome lattice, characterized by two distinct bond lengths within the kagome net. Among them, the simplest examples are La_3Al, $ThAl_3$, and UPt_3, which crystallize in the Ni_3Sn type. These compounds are formed by a simple stacking of A_3B layers, with the A atoms forming the kagome layer. By introducing an additional element at a lattice site of the unit cell, the Ni_3Sn type transforms into the $BaNiO_3$ type, which is unique in that the kagome layer is constructed by anions.

Similar to $BaNiO_3$, the laves-$MgZn_2$ type contains two additional atoms per unit cell and represents the largest noncubic family, comprising 24 superconductors. Substituting some atoms with a third element in the $MgZn_2$ type yields the Mg_2Cu_3Si type, which enhances the two-dimensionality of the kagome network and produces cleaner band structures. Additionally, the laves-$MgNi_2$ type can be regarded as a modification of the laves-$MgZn_2$ type. The most structurally complex kagome superconductors are $BaReH_9$ (high-pressure phase) and $CeIr_3$ (Ni_3Pu type), where up to six kagome layers stack sequentially within a single unit cell.

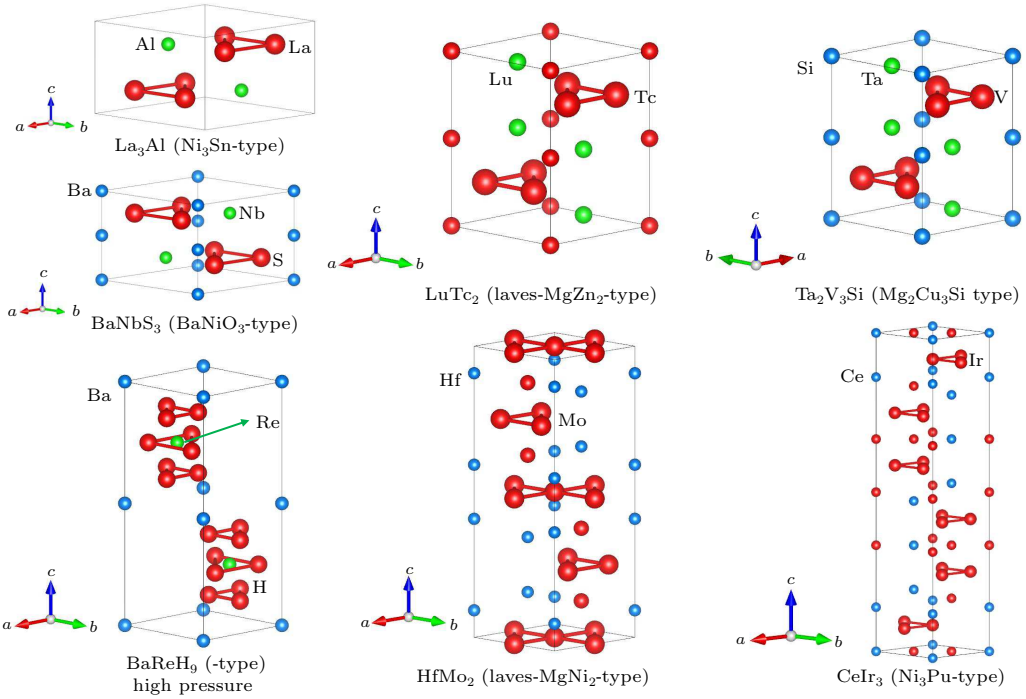


Fig. 4. Crystal structures of superconductors with multiple kagome layers in a unit cell. Red atoms indicate bonded sites within individual kagome planes.

3.1.2. Superconductors with crossed kagome layers

This category comprises superconductors with intersecting kagome layers, where the 2D kagome net forms part of a larger three-dimensional network, typically in cubic systems. Figure 5 shows several representative structures, including the laves-$MgCu_2$, Cu_3Au, spinel-$MgAl_2O_4$, β-pyrochlore-$RbNiCrF_6$, and α-pyrochlore-$Ca_2Nb_2O_7$ types. The interconnected kagome lattices in these cubic superconductors tend to disrupt otherwise clean kagome band structures. Notably, $Cd_2Re_2O_7$, an α-pyrochlore ($Ca_2Nb_2O_7$-type) superconductor, hosts Cd–Re dual-element kagome lattices and exhibits superconductivity with $T_C \approx 0.96$ K.

The superconducting transition temperatures of the various prototypes are shown in Fig. 6(a). Excluding high-pressure data (labeled as triangles), the majority of kagome superconductors exhibit transition temperatures below 10 K, with three notable exceptions: $NbRu_3$ ($T_C \sim 15$ K), $LiTi_2O_4$

($T_C \sim 12.3$ K), and $ScTc_2$ ($T_C \sim 10.9$ K), which are marked as pentagrams in Fig. 6(a). Figure 6(b) shows the element frequency heatmap across T_C bins for all 129 kagome superconductors. It reveals that as the superconducting transition temperature increases, the elemental composition of kagome superconductors becomes more homogeneous and concentrated. The results further indicate that compounds in our database with $T_C > 13$ K display a strong preference for Nb and Ru. Row clustering in the heatmap highlights several major superconducting material families enriched in La, Ru, Os, and Zr.

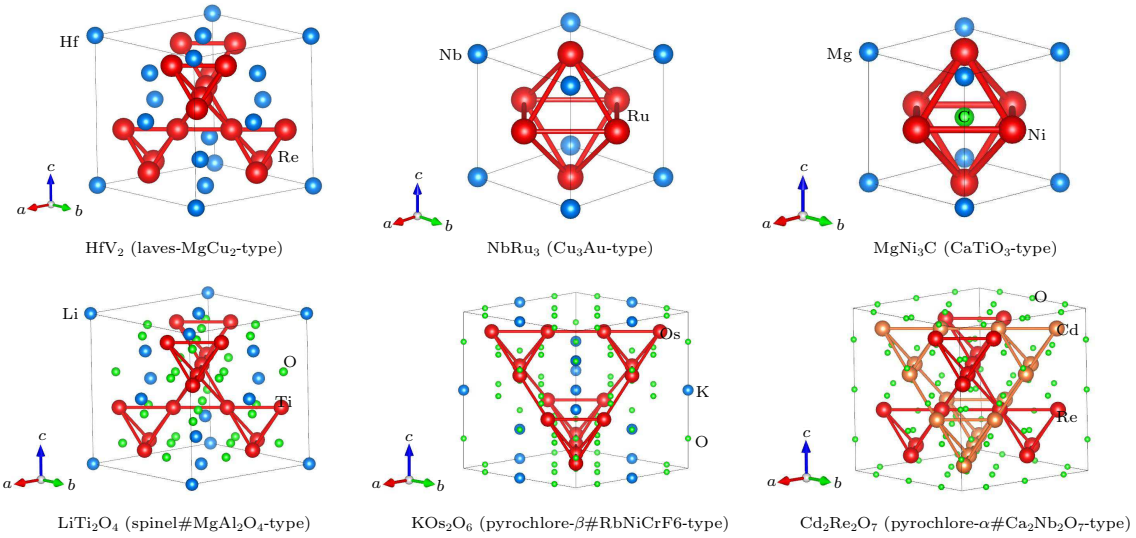


Fig. 5. A 3D crystal structure illustrating intersecting kagome layers. Red atoms indicate shared sites between different kagome planes.

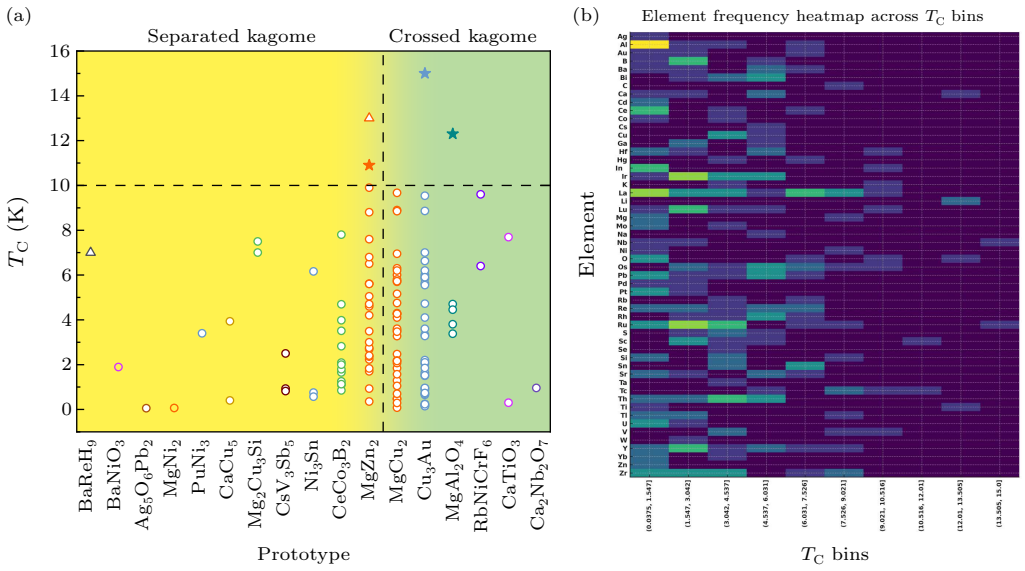


Fig. 6. (a) Critical temperatures (T_C) of 129 kagome superconductors. Ambient-pressure data are shown as circles, high-pressure measurements as triangles, and stars denote materials with $T_C > 10$ K. Colors correspond to materials sharing the same reduced chemical formula. (b) Element frequency heatmap across T_C bins. The elements are listed on the left of the plot. The T_C bin values are determined from the specific transition temperatures in our database. The colors indicate the frequency of elements appearing in each T_C interval, with deep blue representing the lowest frequency and yellow the highest.

3.2. Kagome superconductors with topological flat bands or clean kagome bands

An ideal kagome lattice intrinsically hosts Dirac fermions, flat bands, and van Hove singularities in its electronic structure. The exotic quantum phenomena observed in kagome materials are widely believed to arise from this distinctive band topology.[28,29] In the case of the breathing kagome lattice, a simple tight-binding calculation shows that while topological flat bands persist, the Dirac fermions and van Hove singularities are destroyed.[30,31] Therefore, topological flat bands are also expected to survive in separated kagome lattices, regardless of whether they are breathing or not.

In real materials, however, flat bands are rare and typically appear only in a few systems such as heavy-fermion compounds, kagome lattices, and twisted bilayer graphene. By cross-screening the 129 identified kagome superconductors with the database of topological flat bands,[32] we obtained

eleven kagome superconductors that display nearly ideal flat bands: $BaNbS_3$, La_3Al, Nb_3Si, $CaIr_2$, $CaLi_2$, $ScIr_2$, $SrIr_2$, YIr_2, $ZrAl_2$, $ZrZn_2$, and $SrTiO_3$. Representative band structures ($BaNbS_3$, La_3Al, Nb_3Si, and $CaIr_2$[33]) are shown in Fig. 7, clearly exhibiting the flat-band features (all raw data and plots are available in our database).

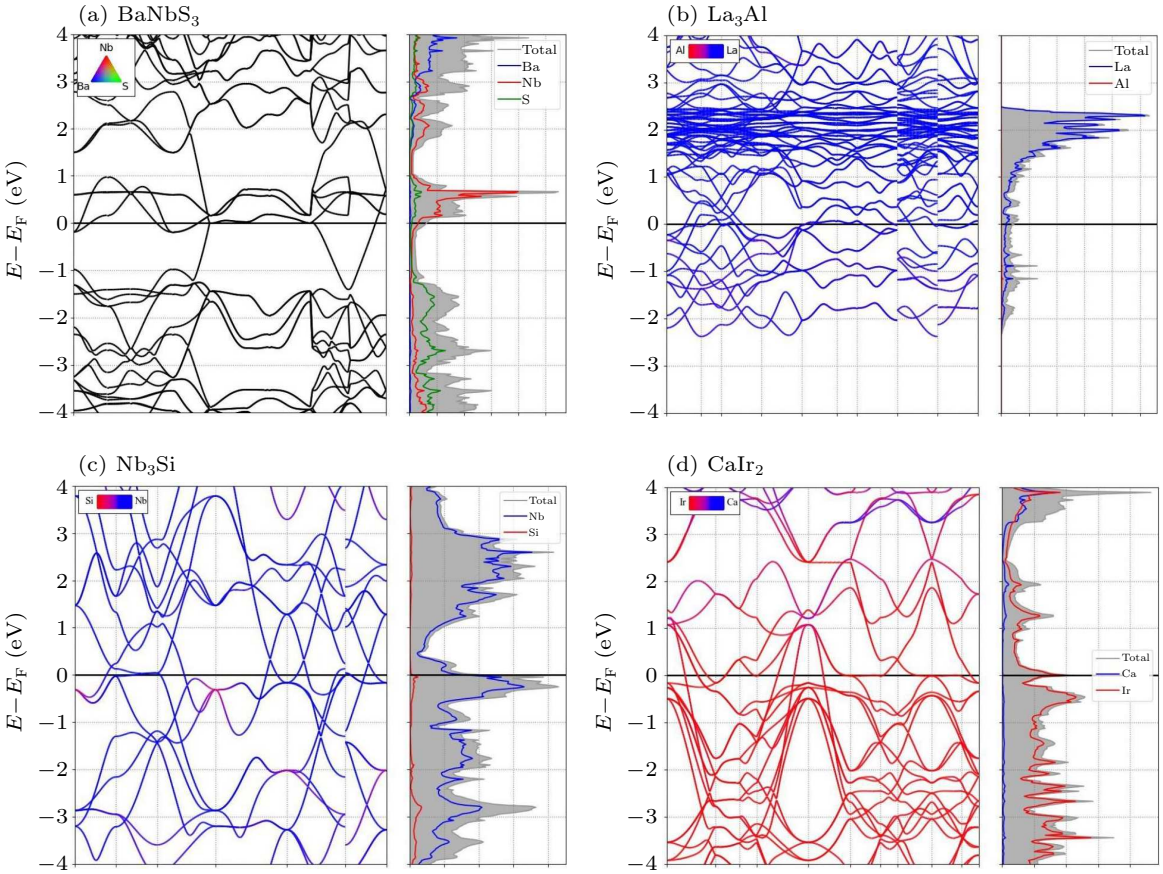


Fig. 7. Band structures of (a) $BaNbS_3$, (b) La_3Al, (c) $CaIr_2$, and (d) $CaLi_2$ showing the presence of flat bands.

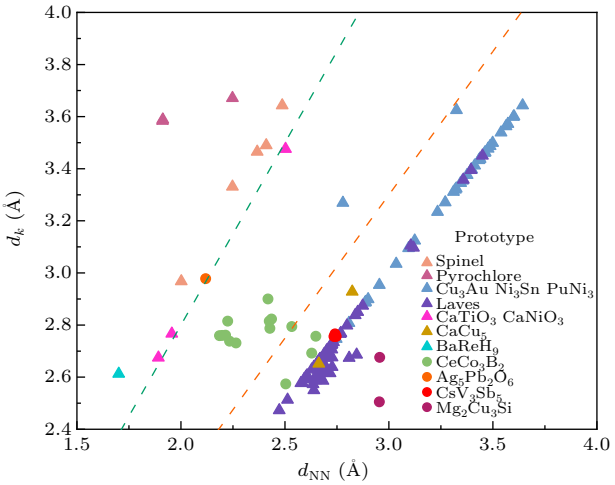


Fig. 8. Classification of kagome superconductors based on interatomic distances (d_K: kagome layer spacing; d_{NN}: nearest-neighbor distance). Triangles indicate systems with coupled kagome lattices that lack discernible kagome band features, while circles indicate systems with well-defined kagome electronic bands.

In the ideal kagome lattice, Dirac points and van Hove singularities are expected. Yet, in real materials, strong interactions with surrounding atoms often distort kagome-derived bands, making it challenging to identify superconductors with clean kagome electronic structures. To tackle this, Jovanovic *et al.*[19] recently proposed a simple chemical rule to distinguish superconductors with clean kagome bands. This rule applies to "isolated" kagome lattices — as opposed to "linked" ones — where "linked" refers to systems containing atoms of the same or chemically similar elements within +0.1 of the kagome bond length ratio or closer.[19] The rule evaluates the kagome–kagome distance (d_K) and the kagome–neighbor distance (d_{NN}), and identifies clean kagome bands when the ratio satisfies $d_K/d_{NN} < 1.1$. As shown in Fig. 8, most superconductors marked by triangles fall into the linked category and lack identifiable kagome bands. By contrast, those marked by circles exhibit clean kagome bands. Although many $CeCo_3B_2$-type compounds fall above the $d_K/d_{NN} > 1.1$ threshold, earlier studies confirmed that they too host clean kagome bands.[19]

Beyond this baseline chemical rule, we introduce additional criteria to further refine the identification of superconductors with clean kagome bands. Since band structures can be disrupted by interactions with non-kagome atoms, and breathing kagome lattices lack Dirac points and van Hove singularities, we exclude superconductors with "crossed kagome" and "breathing kagome" lattices from our dataset.

This filtering reduces the candidate list to roughly 20 materials, which can then be validated by examining their electronic band structures provided in the supporting information. Our results suggest that superconductors of the CsV_3Sb_5, $CeCo_3B_2$, and Mg_2Cu_3Si families consistently exhibit clean kagome bands, indicating that they merit further investigation.

3.3. Kagome superconductors with spin ordering

The coexistence of superconductivity and magnetism in kagome lattices has been recognized in the prototypical material $CeRu_2$.[34] Theoretical studies have particularly focused on the interplay between magnetism and superconductivity in kagome electrons at the van Hove and Dirac fillings. These pioneering investigations have laid the foundation for exploring magnetically intertwined kagome superconductivity. Using magnetic property data from the MP database, non-magnetic materials can be filtered out to identify potential kagome magnetic superconductors. Table 1 provides a list of related materials.

Table 1. Kagome superconductors with possible spin ordering.

Formula	T_C (K)	Total magnetization normalized formula units
$LiTi_2O_4$	12.3	0.5698
V_2CuS_4	4.45	3
$Cd_2Re_2O_7$	0.96	1.1743
$CeIr_3$	3.4	0.0861
UPt_3	0.57	2.0327
$BaRh_2$	6	0.6535
TaV_2	3.6	0.3974
$ZrZn_2$	0.29	1.1035
$CeIn_3$	0.17	1.0235
La_3In	9.54	1.4429
La_3Tl	8.86	1.6388
UAl_3Pd_2	2	2.2051
$MgNi_3C$	7.69	0.5675
$CeRu_2$	6.3	0.0004*

*Experiments proved that it has magnetism, but not supported by the first-principles calculations.

Among the identified superconductors with potential magnetic ordering, some well-known materials stand out, such as $LiTi_2O_4$ (anomalous magnetoresistance[35]), CuV_2S_4 (charge density wave[36]), and UPd_2Al_3 (antiferromagnetic heavy-fermion superconductor[37]). These materials possess correlated and intertwined electronic states similar to the complex behavior observed in CsV_3Sb_5. Further investigations into the interplay between magnetism and superconductivity in these materials will shed light on the time-reversal-symmetry-breaking superconducting ground state predicted in earlier theoretical studies.

3.4. Kagome superconductors with CDW order

Although kagome superconductors with a transition temperature T_C up to 7 K have been known for over half a century, their coexistence with CDW order has only been confirmed in the recently discovered kagome superconductors AV_3Sb_5 (A = K, Rb, Cs). The unusual pair density waves identified in these CDW-hosted superconductors have quickly triggered significant interest in the interaction between CDW order and superconductivity in a kagome lattice. In addition to the AV_3Sb_5 family, several other kagome superconductors are also identified that display CDW ordering above T_C. These include HfV_2 ($T_C \sim 3.6$ K, $T_{CDW} \sim 150$ K), ZrV_2 ($T_C \sim 8.85$ K, $T_{CDW} \sim 120$ K), and CuV_2S_4 ($T_C \sim 4.45$ K, $T_{CDW} \sim 90$ K), all of which belong to the Fd-3m space group at room temperature.

The pristine structure of CsV_3Sb_5 (Fig. 9(b)) is reported to exhibit structural instabilities based on phonon calculations, which are related to the CDW.[38] The tri-hexagonal distortion (Fig. 9(a)) of CsV_3Sb_5 is suggested to produce the CDW, corresponding to a wave vector of (0.5, 0.5, 0.5).[39] However, recent single-crystal diffraction data suggest that the kagome layers of CsV_3Sb_5 exhibit both tri-hexagonal (Fig. 9(a)) and Star of David (Fig. 9(c)) distortions below the CDW phase transition temperature. These distortions change the space group of CsV_3Sb_5 from $P6/mmm$ to P-3 and enlarge the original unit cell, corresponding to a wave vector of (0.5, 0.5, 0.25).[40] Further investigation is required to elucidate the origin of the CDW in CsV_3Sb_5.

The identified HfV_2, ZrV_2, and CuV_2S_4 superconductors belong to the class of materials with interpenetrating kagome planes, and a few studies suggest that CDW ordering may appear in these kagome materials.[41–43] For example, the incommensurate CDW phase transition of CuV_2S_4 is accompanied by a structural phase transition from Fd-3m to $Imm2$ (see Figs. 9(d) and 9(e)), with an incommensurate wave vector of (0.7391, 0.7391).[42] Moreover, the superconducting behavior in CuV_2S_4 remains a subject of controversy,[10,44] and further studies are required to better understand this compound.

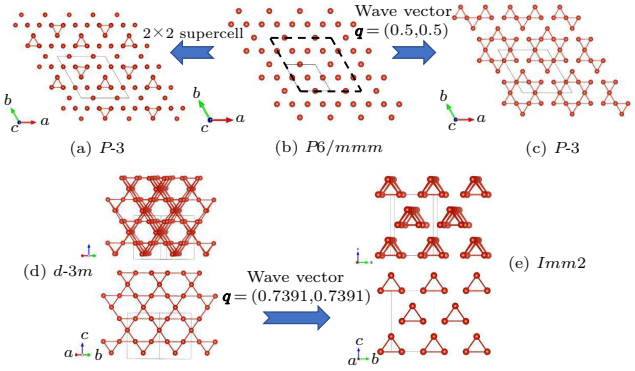


Fig. 9. Crystal structures associated with CDW. Only V atoms are shown for clarity. (a) Tri-hexagonal and (c) star of David distortions for CsV_3Sb_5, adapted from Ref. [38]. Pristine structures of CsV_3Sb_5 (b) and CuV_2S_4 (d). (e) Incommensurate crystal structure of CuV_2S_4, adapted from Ref. [43]. The top shows the original structure, while the bottom is viewed along the [110] direction.

4. Conclusion

Our study introduces a high-throughput computational framework for identifying and categorizing kagome superconductors, combining data from the MP database and the MDR SuperCon Datasheet. By systematically screening over 150000 inorganic materials and 26000 superconductors, we identified 129 kagome superconductors belonging to 17 distinct structural prototypes. These materials exhibit diverse electronic and magnetic properties, including topological flat bands, coexisting CDW orders, and magnetic correlations, providing a rich platform for exploring quantum phenomena and offering critical insights into their structural features, electronic orders, and superconducting mechanisms. The database organizes materials into categories based on structural classification, band topology, and electronic/magnetic orders, enabling rapid screening of candidates for the synthesis of kagome superconductors with tailored properties. This work establishes a foundation for experimental synthesis and theoretical studies, prioritizing high-potential candidates for novel quantum phenomena.

Data availability statement

The data that support the findings of this study are openly available in the Science Data Bank at the following link: https://doi.org/10.57760/sciencedb.25134.

Acknowledgments

The authors would like to thank Prof. Kun Jiang from the IOP, CAS for useful discussions. This work was supported by the National Key Research and Development Program of China (Grant No. 2018YFE0202600), the National Natural Science Foundation of China (Grant No. 52272268), the Key Research Program of Frontier Sciences, CAS (Grant No. QYZDJ-SSWSLH013), the Informatization Plan of Chinese Academy of Sciences (Grant No. CAS-WX2021SF-0102), and the Youth Innovation Promotion Association of CAS (Grant No. 2019005). The AI-driven experiments, simulations and model training were performed on the robotic AI-Scientist platform of Chinese Academy of Sciences.

References

[1] Lin Z, Choi J H, Zhang Q, *et al.* 2018 *Phys. Rev. Lett.* **121** 096401
[2] Ye L, Kang M, Liu J, von Cube F, Wicker C R, Suzuki T, Jozwiak C, Bostwick A, Rotenberg E, Bell D C, Fu L, Comin R and Checkelsky J G 2018 *Nature* **555** 638
[3] Liu D F, Liang A J, Liu E K, *et al.* 2019 *Science* **365** 1282
[4] Teng X, Chen L, Ye F, *et al.* 2022 *Nature* **609** 490
[5] Yin J X, Lian B and Hasan M Z 2022 *Nature* **612** 647
[6] Jiang K, Wu T, Yin J X, Wang Z, Hasan M Z, Wilson S D, Chen X and Hu J 2023 *National Science Review* **10** nwac199
[7] Ortiz B R, Teicher S M L, Hu Y, *et al.* 2020 *Phys. Rev. Lett.* **125** 247002
[8] Song Y P, Ying T P, Chen X, Han X, Wu X, Schnyder A P, Huang Y, Guo J G and Chen X L 2021 *Phys. Rev. Lett.* **127** 237001
[9] Chen X, Zhan X, Wang X, Deng J, Liu X B, Chen X, Guo J G and Chen X L 2021 *Chin. Phys. Lett.* **38** 057402
[10] Seki Y, Hagino T, Takayanagi S and Nagata S 1992 *J. Phys. Soc. Jpn.* **61** 2597
[11] Xu Z, Le T and Lin X 2025 *Chin. Phys. Lett.* **42** 037304
[12] Yan X, Deng H, Yang T, Liu G, Song W, Miao H, Tu Z, Lei H, Wang S and Lin B 2024 *Chin. Phys. Lett.* **41** 097401
[13] Jiang Y, Yu Z, Wang Y, Lu T, Meng S, Jiang K and Liu M 2022 *Chin. Phys. Lett.* **39** 047402
[14] Zhang X, Chen A and Zhou Z 2019 *WIREs Comput. Mol. Sci.* **9** e1385
[15] Regnault N, Xu Y, Li M R, *et al.* 2022 *Nature* **603** 824
[16] Meschke V, Gorai P, Stevanović V and Toberer E S 2021 *Chem. Mater.* **33** 4373
[17] MDR SuperCon Datasheet Version 220808 2022 (Exception: Datasheet)
[18] Jain A, Ong S P, Hautier G, Chen W, Richards W D, Dacek S, Cholia S, Gunter D, Skinner D, Ceder G and Persson K A 2013 *APL Materials* **1** 011002
[19] Jovanovic M and Schoop L M 2022 *J. Am. Chem. Soc.* **144** 10978
[20] Singh H K, Sehrawat A, Shen C, Samathrakis I, Opahle I, Zhang H and Xie R 2023 *Acta Materialia* **242** 118474
[21] Ong S P, Richards W D, Jain A, Hautier G, Kocher M, Cholia S, Gunter D, Chevrier V L, Persson K A and Ceder G 2013 *Computational Materials Science* **68** 314
[22] Jain A, Hautier G, Ong S P, Moore C J, Fischer C C, Persson K A and Ceder G 2011 *Phys. Rev. B* **84** 045115
[23] Wang A, Kingsbury R, McDermott M, Horton M, Jain A, Ong S P, Dwaraknath S and Persson K A 2021 *Sci. Rep.* **11** 15496
[24] Aykol M, Dwaraknath S S, Sun W and Persson K A 2018 *Sci. Adv.* **4** eaaq0148
[25] Horton M K, Montoya J H, Liu M and Persson K A 2019 *npj Comput. Mater.* **5** 64
[26] Munro J M, Latimer K, Horton M K, Dwaraknath S and Persson K A 2020 *npj Comput. Mater.* **6** 112
[27] Kresse G and Furthmüller J 1996 *Comput. Mater. Sci.* **6** 15
[28] Le T, Liu J, Wang Z and Lin X 2024 *Chin. Phys. B* **33** 107402
[29] Liu Y, Li J, Yang W, Lu J, Cao B, Li H, Chai W, Wu S, Li B, Sun Y, Jiao W, Wang C, Xu X, Ren Z and Cao G 2024 *Chin. Phys. B* **33** 057401
[30] Bolens A and Nagaosa N 2019 *Phys. Rev. B* **99** 165141
[31] Sun Z, Zhou H, Wang C, Kumar S, Geng D, Yue S, Han X, Haraguchi Y, Shimada K, Cheng P, Chen L, Shi Y, Wu K, Meng S and Feng B 2022 *Nano Lett.* **22** 4596
[32] Tang F, Ono S, Wan X and Watanabe H 2022 *Phys. Rev. Lett.* **129** 027001
[33] Yu Y, Liu Z, Chen Z, Li Q, Wang Y, Wang X, Gong C, Zhuang Z, Ruan B B, Ren H, Sun P, Guo J G and Jin S 2025 *Chin. Phys. B* **34** 017401
[34] Mielke III C, Liu H, Das D, Yin J X, Deng L Z, Spring J, Gupta R, Medarde M, Chu C W, Khasanov R, Hasan Z M, Shi Y, Luetkens H and Guguchia Z 2022 *J. Phys.: Condens. Matter* **34** 485601
[35] Jin K, He G, Zhang X, Maruyama S, Yasui S, Suchoski R, Shin J, Jiang Y, Yu H S, Yuan J, Shan L, Kusmartsev F V, Greene R L and Takeuchi I 2015 *Nat. Commun.* **6** 7183
[36] Kishimoto Y, Ohno T, Kanashiro T, Michihiro Y, Mizuno K, Miyamoto M, Tanaka T and Miyatani K 1995 *Solid State Commun.* **96** 23
[37] Sato N K, Aso N, Miyake K, Shiina R, Thalmeier P, Varelogiannis G, Geibel C, Steglich F, Fulde P and Komatsubara T 2001 *Nature* **410** 340
[38] Tan H, Liu Y, Wang Z and Yan B 2021 *Phys. Rev. Lett.* **127** 046401
[39] Song B, Ying T, Wu X, *et al.* 2023 *Nat Commun* **14** 2492
[40] Ortiz B R, Teicher S M L, Kautzsch L, Sarte P M, Ratcliff N, Harter J, Ruff J P C, Seshadri R and Wilson S D 2021 *Phys. Rev. X* **11** 041030
[41] Pan V M, Bulakh I E, Kasatkin A L and Shevchenko A D 1978 *Journal of the Less Common Metals* **62** 157
[42] Kawaguchi S, Kubota Y, Tsuji N, Kim J, Kato K, Takata M and Ishibashi H 2012 *J. Phys.: Conf. Ser.* **391** 012095
[43] Kawaguchi S, Ishibashi H, Tsuji N, Kim J, Kato K, Takata M and Kubota Y 2013 *J. Phys. Soc. Jpn.* **82** 064603
[44] Le Nagard N, Katty A, Collin G, Gorochov O and Willig A 1979 *Journal of Solid State Chemistry* **27** 267
[45] Dong Z, Shi L, Wang B, Huo M, Huang X, Huang C, Ma P, Zhang Y, Shen B and Wang M 2024 *Chin. Phys. B* **33** 107102